Environmental Pollution 409 (2026) 128957

Contents lists available at ScienceDirect

Environmental Pollution

journal homepage: www.elsevier.com/locate/envpol

Effects of marine heatwaves and marine cold spells on toxin production in *Alexandrium catenella*

Paola A. Villanueva [a,b,c], Carlos Lara [d,*], Jorge M. Navarro [b,c], Nelson Valdivia [b,c], Elisabeth Teca [d], Amália M.S. Detoni [e], Gonzalo S. Saldías [f,g], Pamela Carbonell [h], Luis Norambuena [h], Patricio A. Díaz [i,j], Bernardo R. Broitman [k,l]

[a] *Programa de Doctorado en Ciencias de la Acuicultura, Universidad Austral de Chile, Puerto Montt, Chile*
[b] *Instituto de Ciencias Marinas y Limnológicas, Universidad Austral de Chile, Valdivia, Chile*
[c] *Centro FONDAP de Investigación en Dinámica de Ecosistemas Marinos de Altas Latitudes (IDEAL), Universidad Austral de Chile, Valdivia, Chile*
[d] *Departamento de Ecología, Universidad Católica de la Santísima Concepción, Concepción, Chile*
[e] *Institut des Substances et Organismes de la Mer, Nantes Université, Nantes, France*
[f] *Departamento de Física, Facultad de Ciencias, Universidad del Bío-Bío, Concepción, Chile*
[g] *Centro de Investigación Oceanográfica COPAS Coastal, Universidad de Concepción, Concepción, Chile*
[h] *Centro de Estudios de Algas Nocivas (CREAN), Instituto de Fomento Pesquero (IFOP), Puerto Montt, Chile*
[i] *Centro i-mar, Universidad de Los Lagos, Puerto Montt, Chile*
[j] *Centro Interdisciplinario para la Investigación Acuícola - Investigación Aplicada (INCAR2), Universidad de Concepción, Concepción, Chile*
[k] *Departamento de Ciencias, Facultad de Artes Liberales, Universidad Adolfo Ibañez, Viña del Mar, Chile*
[l] *Instituto Milenio en Socio-Ecología Costera (SECOS), Santiago, Chile*

ARTICLE INFO

Keywords:
Harmful Algal Blooms
Paralytic shellfish toxins
Toxic components
Alexandrium catenella
Climate change

ABSTRACT

Marine heatwaves (MHWs) and marine cold spells (MCSs) are increasing in frequency and intensity, emerging as major climate-driven stressors in coastal ecosystems. In northern Patagonia, these thermal extremes have been associated with shifts in plankton communities and an increasing incidence of harmful algal blooms (HABs), particularly those dominated by *Alexandrium catenella*, the main producer of paralytic shellfish toxins (PSTs) in Chile. However, the physiological responses of HAB species to thermal extremes remain poorly understood, limiting their use as ecological indicators of HAB risk under climate variability. We experimentally evaluated the effects of simulated MHWs and MCSs on cell density, pigment concentration and toxin production in a monoclonal *A. catenella* strain isolated from northern Patagonia. Extreme thermal treatments were imposed using progressive temperature changes of +1 °C day^{-1} to 16 °C for the MHW treatment and −1°C day^{-1} to 8 °C for MCSs treatment, followed by two exposure–recovery cycles, followed by two exposure–recovery cycles. Responses were assessed by quantifying cell density, pigment content, and PST composition (neoSTX, STX, GTX2/3, GTX4/1). MHW exposure promoted transient increases in cell density and significantly enhanced cellular toxin quotas, particularly GTX2/3. In contrast, MCSs produced contraction–recovery dynamics in population size with moderate effects on toxin profiles. Multivariate analyses (PERMANOVA) revealed significant temporal variation, across exposure–recovery cycles. Overall, our results demonstrate that simulated thermal extremes can modify cell density and toxin production in *A. catenella*, with MHW-like conditions intensifying toxin production and altering toxic profiles.

1. Introduction

Marine heatwaves (MHWs) and marine cold spells (MCSs) are currently the more visible manifestations of climate change in the ocean (Pujol et al., 2022; Smale et al., 2019; Hobday et al., 2016). MHWs are characterized by sea surface temperatures exceeding the 90th percentile of local climatology for prolonged periods (at least 5 days to several weeks), whereas MCSs represent sustained cold anomalies below the 10th percentile (Hobday et al., 2016; Schlegel et al., 2017). Situated at opposite ends of the thermal spectrum, MHWs and MCSs are protracted pulse disturbances that can represent strong ecological stressors (Smith et al., 2023) with severe impacts on marine ecosystems (Holbrook et al., 2019). The intensity and duration of MHWs and MCSs can alter local to regional patterns of planktonic community structure,

* Corresponding author.
E-mail address: carlos.lara@ucsc.cl (C. Lara).

https://doi.org/10.1016/j.envpol.2026.128957
Received 16 March 2026; Received in revised form 31 July 2026; Accepted 13 August 2026
Available online 2 September 2026

including changes in the abundance and composition of harmful or toxic phytoplankton species (Garrabou et al., 2022; Oliver et al., 2021; Dias et al., 2025). In northern Patagonia, on the west coast of South America (40–45°S), both MHWs and MCSs have recently increased in intensity and duration, triggering changes in stratification, vertical mixing, and nutrient availability along the region (Pujol et al., 2025). These physical changes can alter phytoplankton community structure by shifting the abundance and composition of dominant functional groups, as well as their biomass dynamics (Cuevas et al., 2019; Poblete-Ulloa et al., 2024).

Northern Patagonia has experienced an increasing number of harmful algal blooms (HABs) during years of extreme thermal anomalies, suggesting a direct link between climate variability and the proliferation of toxic species (Díaz and Figueroa, 2023; Marquet et al., 2024). Thus, understanding how thermal extremes affect HABs–forming species (e.g. changes in cell density or toxicity) may provide useful insights into the potential responses of HAB dynamics under future climate scenarios (Burgh-Day et al., 2022).

The ecosystem changes following extreme thermal events have been linked to substantial impacts in communities reliant on coastal fisheries and aquaculture (Smith et al., 2021). Similarly, HABs outbreaks generate significant economic and ecological impact that are often difficult to quantify (Rodríguez et al., 2011; Avdelas et al., 2021; Díaz and Álvarez, 2023). In northern Patagonia, HABs outbreaks affecting humans and other consumers of toxic shellfish have been repeatedly associated with climatic and environmental anomalies (e.g., Lara et al., 2016; Garreaud, 2018; León-Muñoz et al., 2018; Díaz et al., 2023, 2025). These coupled anomalies have also coincided with marked declines in the availability of wild mussel larvae and juvenile (seed), leading to cascading impacts on mussel aquaculture production and regional economies (Molinet et al., 2025). This social-ecological connection underscores the need to integrate biophysical processes with human dimensions when assessing ecosystem vulnerability (Van Dolah et al., 2016). Collectively, the linkage between extreme environmental events and negative social-ecological effects highlights the need for fundamental research to better understand HAB-related risks under future environmental change and to support the sustainable use of coastal marine resources (Pinillos and Ruiz, 2024).

Alexandrium catenella is the main dinoflagellate producer of paralytic shellfish toxins (PSTs) in Chile (Barría et al., 2022; Díaz and Figueroa, 2023; Díaz et al., 2024), which comprise a diverse group of toxin analogues differing markedly in toxicity and whose composition can vary under different environmental conditions (Shimizu, 1996; Cembella, 1998; Wiese et al., 2010). The northern expansion of *A. catenella* over the past five decades has resulted in human poisoning (> 500 people), prolonged fishery closures across extensive geographic areas (up to 500 km of coastline), and severe economic losses, particularly for shellfish fishers and the mussel aquaculture industry (Hernández et al., 2016; Navarro et al., 2022; Díaz et al., 2024; Villalobos et al., 2025). The physiology of *A. catenella* is regulated by multiple environmental factors, including temperature, salinity, light intensity, nutrients, turbulence and stratification (Aguilera-Belmonte et al., 2013; Avila et al., 2015; Navarro et al., 2006; Bill et al., 2016). Under stable conditions, northern Patagonian strains of *A. catenella* exhibit growth optima between 10–16°C (Navarro et al., 2006), with toxicity varying according to nutritional status and cellular C:N balance (Han et al., 2016). The temperature change associated with MHWs can strongly affect phytoplankton photophysiology by reducing the maximum quantum yield (Fv/Fm) and increasing the production of reactive oxygen species (ROS), leading to oxidative damage and metabolic stress (Deschaseaux et al., 2019; Zhu et al., 2023). Under these conditions, some microalgae upregulate toxin synthesis as a stress-mitigation strategy, whereas others reduce toxin production due to its high energetic cost (Chakraborty et al., 2019; Bui et al., 2024). Phenological shifts represents another anticipated to warming (Wells et al., 2015). For instance, Moore et al. (2008) predicted an expansion of the developmental window of opportunity for *A. catenella* in Puget Sound, USA, under future climate scenarios. These authors demonstrated that the period in which *A. catenella* bloom occurs annually may also expand because of climate change, specifically by an increase in water temperature. In contrast, MCSs induce metabolic deceleration, reduced cell division rates, and shifts in carbon allocation toward nitrogen-containing compounds, all of which can modify toxin profiles (Kim et al., 2021). Despite this, the effects of marine cold spells on toxic dinoflagellates remain far less understood than those of warming.

Although hot and cold thermal extremes have been documented in northern Patagonia, together with the large socioeconomic impacts of HABs, no studies have simultaneously evaluated the responses of *A. catenella* to both MHW and MCS conditions (Pujol et al., 2022; Oliver et al., 2021; Pujol et al., 2025). Most experimental work to date relies on static thermal gradients that do not capture the intensity, rate of change, or transient nature of real extreme events (Thompson et al., 2013; Ritger and Hofmann, 2025). This gap limits our ability to anticipate how this toxic dinoflagellate will respond under future climate scenarios in which seawater temperature anomalies of +4–5°C and –4–5°C are projected to become increasingly common (Pujol et al., 2025). In this study, we evaluated the effects of simulated MHW and MCS temperature dynamics on cell density and toxin production in *A. catenella*.

2. Methods

2.1. Culture conditions of A. catenella

A monoclonal culture of *A. catenella* originally isolated in 2011 from Coldita Island, Chiloé, Los Lagos Region, Chile (Fig. 1), was used for experimental work. Cultures were maintained in 0.45 μm-filtered seawater enriched with L1 medium (Guillard, 1995) under controlled temperature (12°C), salinity (32 PSU), photoperiod (14:10 h light:dark), and light intensity (59.12 ± 1.12 μmol m^{-2} s^{-1}). Light and photoperiod were controlled using LED tubes suspended above each culture bottle. The dinoflagellate population was propagated in an exponential growth phase and used directly for experimental treatments. Culture bottles were rotated every three days. Each 5-L experimental bottle contained 4800 mL of fresh L1 medium and was inoculated with 200 mL of starter culture at approximately 8000 cells mL^{-1}. This inoculum contained approximately 1.6×10^6 cells and resulted in an initial post-inoculation density of approximately 320 cells mL^{-1} in a final volume of 5 L

2.2. Experimental design

To assess the effects of temperature dynamics on *Alexandrium catenella*, we employed a two-way factorial design with "condition" (three levels: MHW, MCS, and control) and "exposure phase" (four levels: first exposure, first recovery, second exposure, and second recovery) as fixed and crossed factors. Three independent biological replicates (5-L culture bottles used as experimental units) were used for each treatment.

For the MHW treatment, temperature was increased from the control level (12°C) at a rate of 1°C day^{-1} until reaching 16°C. This temperature corresponds to the threshold commonly associated with marine heatwave conditions in northern Patagonia (Pujol et al., 2022). For the MCS treatment, temperature was decreased from the control level at the same rate until reaching 8°C, representing a significant negative thermal anomaly relative to the regional mean temperature (Narváez et al., 2019; Saldías et al., 2021). Control cultures were maintained at a constant 12°C, corresponding to the regional mean sea surface temperature of northern Patagonia. The temperature-change rate of ±1°C day^{-1} was selected to impose a gradual thermal transition and avoid an abrupt temperature shock. Because regional in situ information on natural MHW and MCS ramping rates is limited, this rate

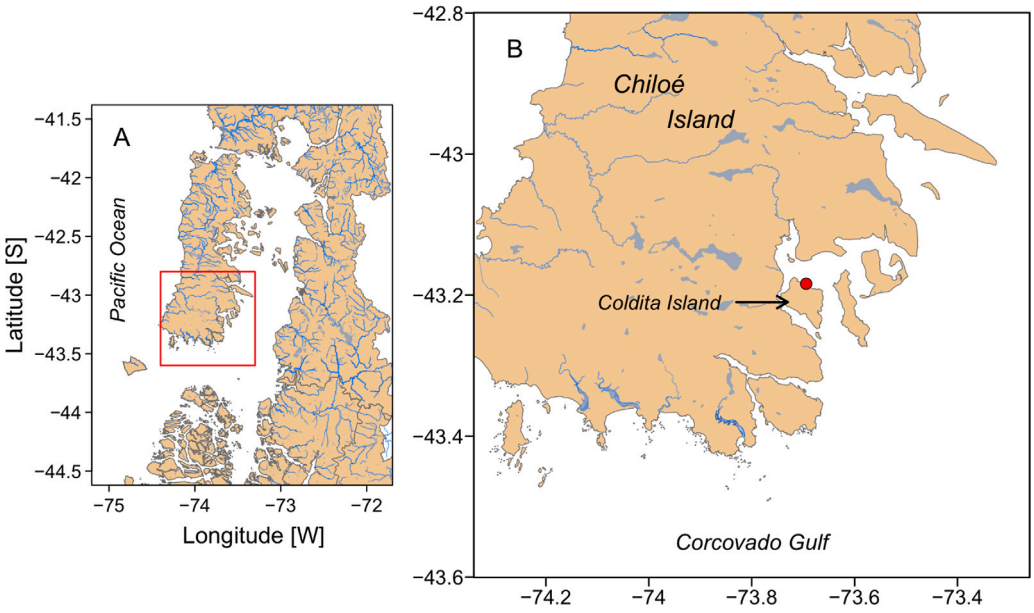

Fig. 1. Coldita Island, Los Lagos, southern Chile. Monoclonal *Alexandrium catenella* cultures were collected from Coldita Island and isolated in 2011.

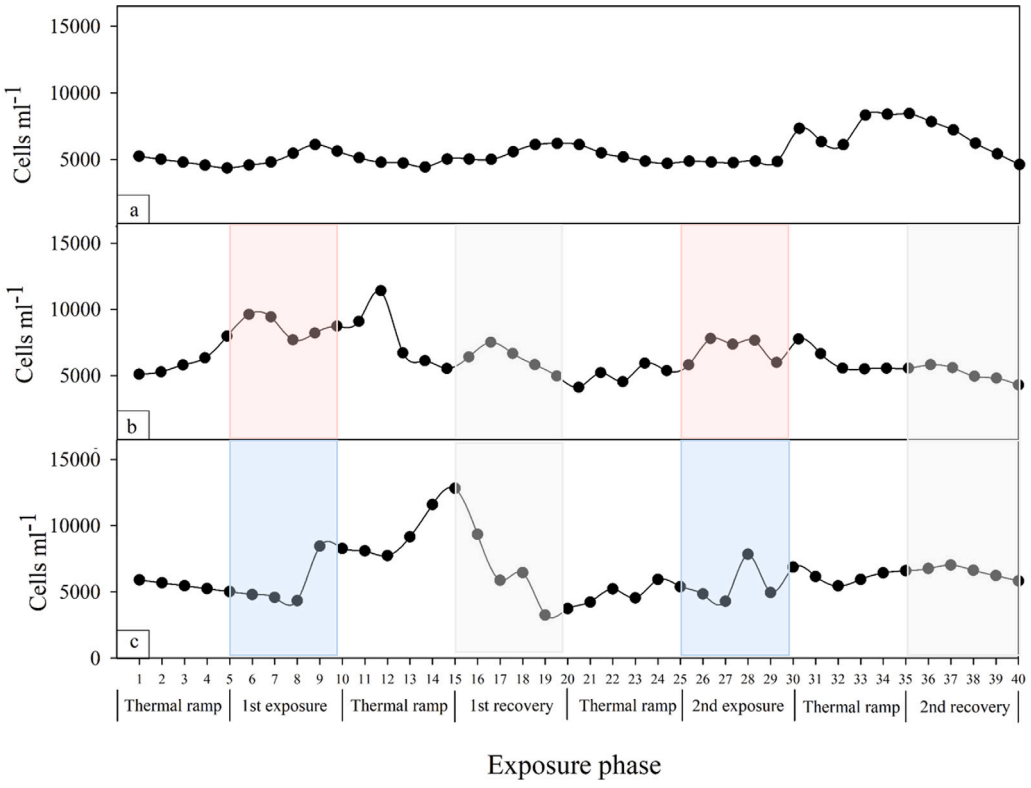

Fig. 2. Growth dynamics of *Alexandrium catenella* under control conditions and simulated thermal extremes. Panels show (a) control treatment, (b) marine heatwave (MHW) exposure, and (c) marine cold spells (MCS) exposure. Red shading indicates thermal exposure phases (warming or cooling), blue shading denotes cold-spell exposure, and gray shading represents recovery periods between successive exposure cycles. (For interpretation of the references to color in this figure legend, the reader is referred to the web version of this article.)

represents an experimental setting rather than an exact reconstruction of a specific regional event.

Once the target temperatures were reached, cultures were maintained under MHW or MCS conditions for an additional five days (first exposure). Temperature was then gradually returned to the control level (12°C) at the same ramping rate and maintained for five days (first recovery). All cultures were supplemented with L1 nutrients before the second exposure–recovery cycle, following the same procedure across the control, MHW, and MCS treatments. The same thermal protocol was subsequently repeated, consisting of a second exposure phase followed by a second recovery phase. Each thermal treatment comprised a complete exposure–recovery scenario, including progressive warming or cooling, maintenance at the target temperature, and subsequent recovery to 12°C. The experiment was designed to evaluate the integrated

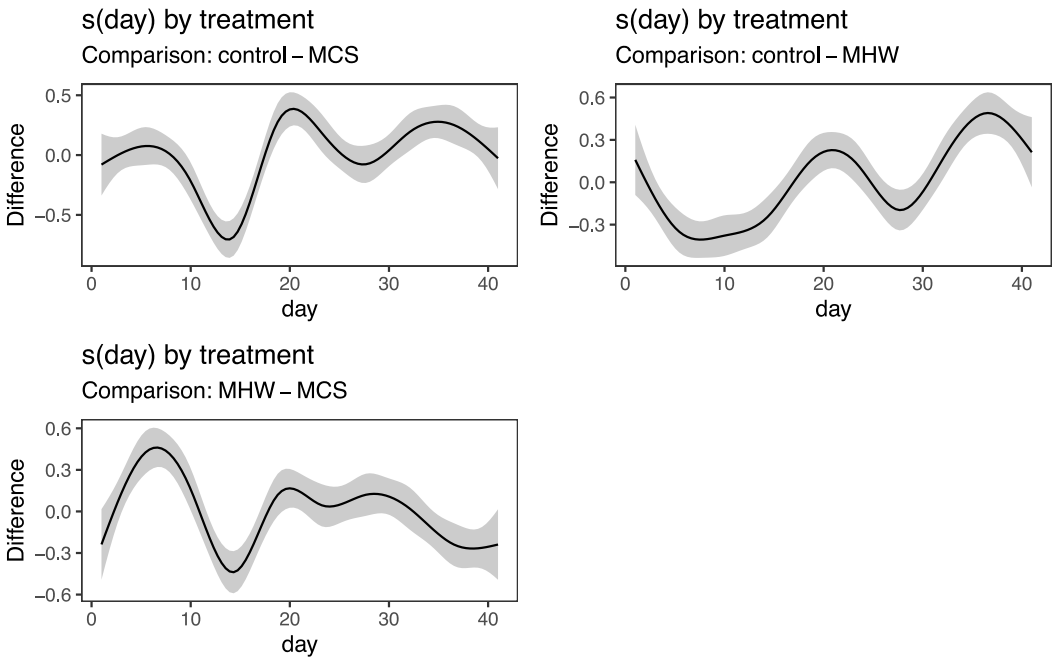

Fig. 3. Pairwise comparisons between experimental treatment over time, after GAM fitted to cell number data. The solid line shows the predicted mean difference of cell number, and the ribbon 95% the confidence interval. Values above (below) zero indicate significantly positive (negative) between-group differences.

response to these thermal scenarios rather than to separate the effects of the ramping and target-temperature phases.

Toxin and chlorophyll samples were collected after five days under each exposure and recovery phase, as well as from the control treatment. The 5-L culture bottles constituted the experimental units throughout the study. Temperature treatments were conducted using climate-controlled chambers equipped with temperature-regulated water baths. This setup allowed the maintenance of control conditions as well as the implementation of the dynamic warming and cooling scenarios described above.

2.3. Cell counts

For quantitative analyses of *A. catenella* cells, 5 mL of the unconcentrated 5% formalin-fixed samples (from each experimental unit) were left to sediment for at least 4 h and analyzed under an inverted microscope (Leica, model DMIL) using the method described by Utermohl (1958). The detection level using this method was 200 cells L^{-1} (i.e., one cell detected after examination of the entire surface of the sedimentation chamber base-plate).

2.4. Chlorophyll-a concentration

For chlorophyll-*a* and pheopigments determination, 50 mL of culture from each experimental unit were filtered in triplicate using 25 mm GF/F filters (0.7 μm nominal pore size). Filters were labeled, wrapped in aluminum foil, and stored at –20°C until further analysis. Pigments were extracted following the protocol of Parsons and Maita (1984). Thus, each filter was placed in a glass tube with 8 mL of 90% acetone (v/v) and kept in darkness at 5°C for 20 h. Samples were then analyzed in a Turner Designs TD-700 fluorometer. After chlorophyll-*a* determination, 100 μL of 2N HCl was added to each sample to quantify the pheopigments.

2.5. Toxin analysis

2.5.1. Sample preparation

Toxin analyses were performed on 36 experimental samples corresponding to the three conditions, four exposure–recovery stages, and three biological replicates. In addition, three samples from the initial culture were analyzed prior to the experimental treatments to characterize the baseline toxin profile, resulting in a total of 39 analyzed samples. Each sample was filtered through 25 mm GF/F filters and stored in Eppendorf tubes with 0.8 mL of 0.05 M acetic acid added to each tube. For cell lysis, we added Lysing Matrix D beads (MP Biomedicals) and processed the samples for 45 s in a Mini-BeadBeater at room temperature. Extracts were then filtered through 0.22 μm PVDF syringe filters and used for analysis by UHPLC–MS/MS.

2.5.2. Reagents and chemicals

Certified reference standards for PSP toxins (C1, C2, GTX1, GTX4, GTX2, GTX3, GTX5, GTX6, dcGTX2, dcGTX3, dcSTX, STX, dcNEO, NEO) were obtained from the National Research Council of Canada (NRCC, Halifax, Canada). LC-MS grade acetonitrile and methanol, formic acid, and glacial acetic acid were obtained from Merck (Darmstadt, Germany). Ammonium formate LC/MS grade was obtained from Fisher Scientific (Belgium). High-purity water was produced with a Milli-Q system (Millipore).

2.5.3. Analysis of toxin components

Acetic acid extracts were diluted 1:4 with acetonitrile and analyzed by HILIC UHPLC–MS/MS using an Agilent Infinity II UHPLC system. PSTs were separated with an Acquity UHPLC BEH amide column (100 × 2.1 mm, 1.7 μm particle size). Chromatographic and MS/MS conditions followed Rodriguez et al. (2018). Capillary voltage was set to 3 kV in negative mode and 3.5 kV in positive mode, with a gas flow of 10 L min^{-1}, gas temperature of 300°C, and nebulizer pressure of 30 psi. The quantification of all paralytic toxins was performed using an external calibration curve of at least 6 points that must meet an R^2 greater than 0.98. Limits of Detection (LOD), Limits of Quantification (LOQ) and calibration range of the toxins studied were shown in Table 1. The analytical procedure followed the validated method described by Rodriguez et al. (2018). Independent quality assurance assessments, including spike recovery, matrix-effect evaluation, procedural blanks, and repeatability tests, were not performed for the present sample set. Therefore, the reported limits of detection (LOD), limits of quantification (LOQ), and calibration performance characterize the analytical performance of the instrument used in this study but should not be interpreted as a complete matrix-specific method validation.

Table 1
LOD, LOQ and calibration range of the toxin calibration curve.

Toxins	LOD nmol L^{-1}	LOQ nmol L^{-1}	Calibration range nmol L^{-1}
C1	7.7	25.6	25.6–1636.4
C2	2.3	7.6	7.6–489.2
dcGTX2	6.8	22.6	22.6–1446.0
dcGTX3	2.0	6.7	6.7–428.0
dcNEO	2.1	6.9	6.9–438.7
dcSTX	4.5	14.9	14.9–955.0
GTX2	7.0	23.2	23.2–1484.1
GTX3	2.9	9.8	9.8–628.7
GTX1	3.9	12.9	12.9–828.4
GTX4	1.2	4.1	4.1–260.2
GTX5	3.8	12.6	12.6–804.8
GTX6	5.6	18.8	18.8–1200
NEO	4.5	14.9	14.9–956.1
STX	4.5	15.0	15.0–960.2

2.6. Statistical analyses

A general additive model (GAM) was used to compare the microalgal temporal dynamics between control, MHW, and MCS treatments. A Tweedie distribution of errors with log link was assumed, based on diagnostic plots such as QQ plots and residuals-vs.-fitted-values plots. The model included microalgal cell count as response variable, and treatment and the treatment-dependent smooth of time as explanatory variables. Further diagnostic test indicated that the basis dimension (k) of each experimental group was apropriate ($p > 0.9$). In addition, the degree of autocorrelation in the model residuals was assessed by means of Pearson product-moment correlations (r). The autocorrelation function detected significant correlations only at a lag of 3 d ($r = -0.35$) and 6 d ($r = 0.24$).

Differences in *A. catenella* toxin profiles among MHW, MCS, and control treatments were assessed using permutational multivariate analysis of variance (PERMANOVA) based on Euclidean distance matrices calculated from toxin concentrations (GTX2/3, GTX4/1, STX, and neoSTX). PERMANOVA was performed using 999 permutations, testing condition (MHW, MCS, or control), exposure phase (first exposure, first recovery, second exposure, or second recovery), and their interaction as fixed factors. Permutations were constrained within experimental units to account for the repeated-measures structure of the design. Similarity percentage (SIMPER) analysis was subsequently used to identify the toxin analogues contributing most to the observed dissimilarities among treatments.

Chlorophyll-*a* and pheopigment concentrations were analyzed separately using linear mixed-effects models (LMMs), with condition and exposure phase included as fixed crossed factors and experimental unit (5-L culture bottle) included as a random intercept. When random-effect variance approached zero, the random-effect structure was removed and the models were refitted as standard linear models (LMs) to avoid over-parametrization and model singularity. Model assumptions were evaluated using quantile–quantile plots and residual-versus-fitted value diagnostics. For pheopigment concentrations, a square-root transformation substantially improved model fit and residual distributions.

The statistical significance of fixed effects was evaluated using Type III ANOVA tests. When significant effects were detected, post hoc comparisons were performed using Tukey-adjusted estimated marginal means to evaluate (i) temporal changes among exposure and recovery phases within each treatment and (ii) differences among treatments within each experimental phase. All statistical analyses were conducted in R version 4.5.2, using the packages vegan, lme4, lmerTest, DHARMa, and emmeans.

3. Results

3.1. Cell growth and toxin component profile in Alexandrium catenella

Under control conditions (constant 12°C), cell cultures exhibited typical growth dynamics through out the 41-day experimental period. Cell density followed a characteristic sigmoidal trajectory, with the lowest density observed on day five (mean ± SEM = 4351 ± 174 cells mL^{-1}) and the highest on day 36 (8441 ± 84 cells mL^{-1}). The growth curve displayed four distinct phases: (i) a lag phase (days 1–5), during which cell population densities remained relatively stable between 5234 ± 366 and 4351 ± 174 cells mL^{-1}; (ii) an exponential phase (days 6–20), with densities increasing from 4577±229 to 6200±403 cells mL^{-1}; (iii) a stationary phase (days 31–36), where peak values ranged from 7324±769 to 8441±84 cells mL^{-1}; and (iv) a decline phase (days 37–41), marked by a reduction to 4615 ± 277 cells mL^{-1} (Fig. 2a).

Exposure to MHW conditions induced rapid but transient changes in cell population dynamics. During the early phase (days 1–10), cell densities ranged from 5101 ± 357 and 8736 ± 240 cells mL^{-1}. The first heat exposure (days 11–14) triggered a sharp increase in population density, peaking at 11,405 ± 285 cells mL^{-1} on day 12; however, this increase was short-lived, followed by a rapid decline to 6122 ± 416 cells mL^{-1} on day 14. The post-exposure recovery phase (days 15–27) was characterized by oscillatory dynamics, with cell densities varying between a minimum of 4115 ± 88 cells mL^{-1} on day 21 and maximum of 7802 ± 203 cells mL^{-1} on day 27. Population responses during the second heat exposure (days 28–31) were more subdued than during initial event, with densities ranging from 5991 ± 521 cells mL^{-1} on day 30 to 7766 ± 714 cells mL^{-1} on day 31. The experiment concluded with a decline in cell densities (days 32–41), stabilizing at approximately 4300 ± 43 cells mL^{-1} (Fig. 2b).

Under MCS conditions, cell populations exhibited complex dynamics characterized by alternating phases of decline and recovery. During the initial growth period (days 1–10), cell densities fluctuated substantially between 5901 ± 389 and 8270 ± 1241 cells mL^{-1}. The first cold exposure (days 11–14) resulted in a contraction of population size to 7730 ± 2242 cells mL^{-1} on day 12, followed by rapid recovery to 11,590 ± 661 cells mL^{-1} on day 14. A pronounced decline occurred during the subsequent recovery period (days 15–27), with densities decreasing from a peak of 12,809 ± 474 to 4290 ± 202 cells mL^{-1}. The second cold exposure (days 28–31) elicited a moderate response, with densities decreasing to 4946 ± 40 cells mL^{-1} on day 29 and recovering to 6155 ± 320 cells mL^{-1} by day 31. During the final phase of the experiment (days 32–41), populations initially recovered from 5446 ± 365 to 7027 ± 105 cells mL^{-1} by day 37, before declining again to 5427 ± 98 cells mL^{-1} at the end of the experiment (Fig. 2c).

In line with these observations, GAM identified complex and statistically significant temporal trends (effective degrees of freedom for control, MHW, and MCS: 7.2, 6.6, and 8.2, respectively). Across time, mean cell number of MHW and MCS was ca. 16% and 11% greater than control, respectively ($p < 0.001$). Pairwise comparisons showed that cell number was significantly lower in control than MWH between day 5 and 15 approximately. Cell number was statistically lower in control than MCS at day 5 approximately (Fig. 3). For both comparisons, we observed oscillating differences starting at day 20 (Fig. 3). In addition, cell number was greater MHW than MCS at day 5–9, but lower at day 15 (Fig. 3). The model accounted for 71% of the variation in cell count ($R^2 = 0.71$) and 87.5% of the deviance.

Four toxic components were identified in the *A. catenella* strain, with an average toxin content of 35.4 fmol $cell^{-1}$. Among the identified components, GTX2/3 was the dominant toxin, reaching 25.72 ± 3.27 fmol $cell^{-1}$, followed by GTX4/1 (7.98 ± 1.87 fmol $cell^{-1}$), neoSTX (1.24 ± 0.40 fmol $cell^{-1}$), and STX (0.50 ± 0.06 fmol $cell^{-1}$) (Fig. 4).

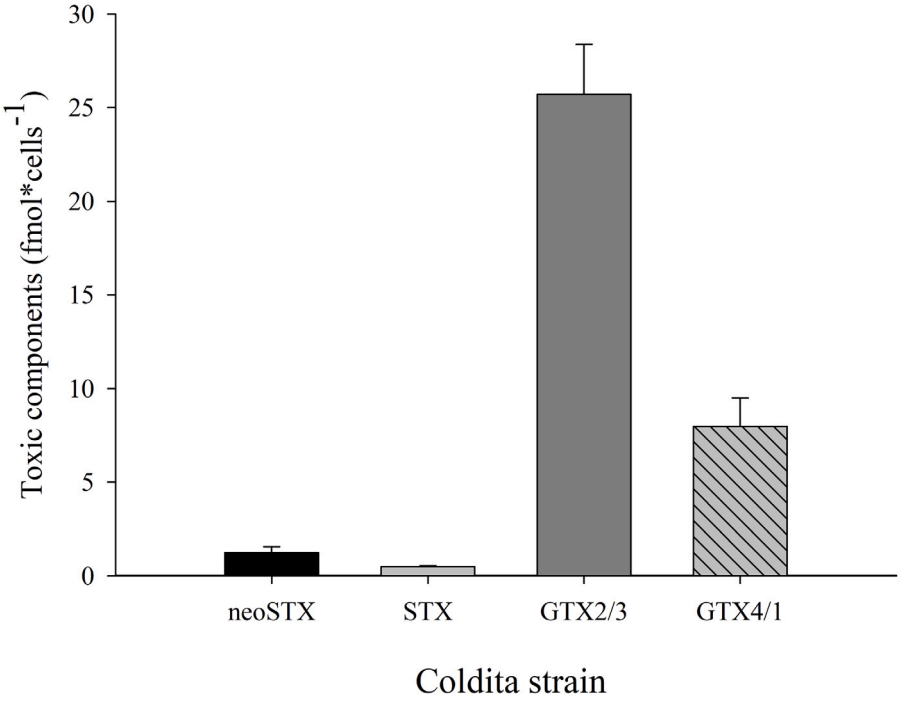

Fig. 4. Toxin profile of the Coldita strain of *Alexandrium catenella*. Different shades of gray represent individual toxin analogues. Bar heights indicate mean toxin concentrations, and error bars denote the standard error (SE).

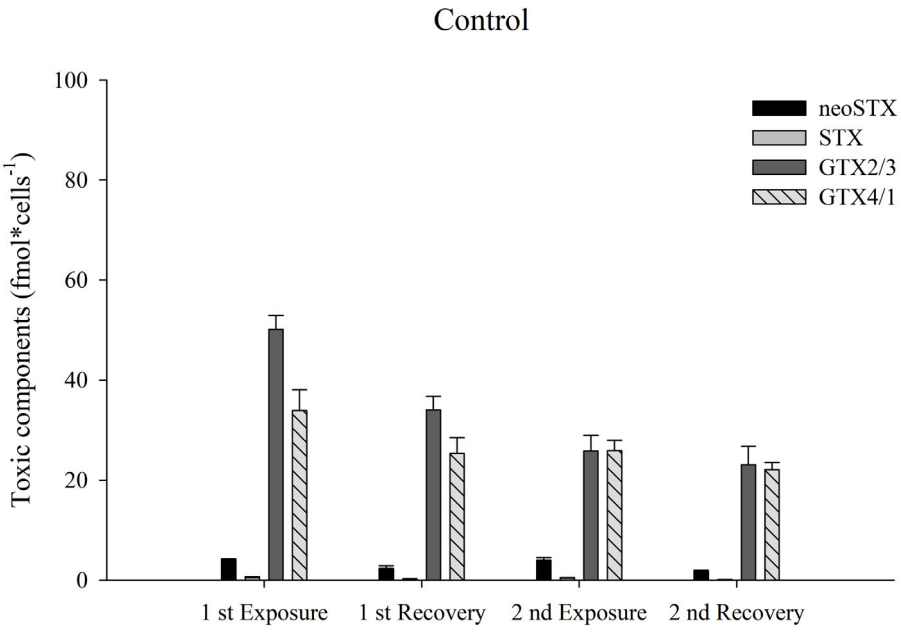

Fig. 5. Toxics components of *Alexandrium catenella* under control conditions. Cellular toxin concentrations (fmol * cell^{-1}) of neoSTX, STX, GTX2/3 and GTX4/1 during two exposure–recovery cycles are depicted. Bar heights indicate mean values and error bars denote the standard error (SE).

3.1.1. Toxin profile of A. catenella in response to MHWs and MCSs

Across all treatments (MHWs, MCSs, and control), *A. catenella* exhibited a consistent toxin profile composed of GTX2/3, GTX4/1, neoSTX, and STX. During the first exposure to MHWs, GTX2/3 reached the highest concentration, meaning 81.98 ± 4.69 fmol cells^{-1}, followed by GTX4/1 (34.60 ± 5.83 fmol cell^{-1}), neoSTX (3.39 ± 0.88 fmol cells^{-1}), and STX (0.66 ± 0.08 fmol cells^{-1}). During the subsequent recovery phase, toxin concentrations decreased while maintaining the same relative composition, with GTX2/3 at 37.23 ± 7.35 fmol cells^{-1}, GTX4/1 at 21.08 ± 3.30 fmol cells^{-1}, neoSTX at 2.65 ± 0.68 fmol cells^{-1}, and STX at 0.36 ± 0.05 fmol cell^{-1}. In the second MHW exposure, the total toxin content further declined compared to the first exposure, although GTX2/3 reassessed the dominant component (26.19 ± 5.26 fmol cell^{-1}), followed by GTX4/1 (21.41 ± 3.50 fmol cell^{-1}), neoSTX (3.01 ± 0.66 fmol cell^{-1}) and STX (0.34 ± 0.08 fmol cell^{-1}) During the final recovery phase, toxin production increased slightly, with GTX2/3 reaching 36.03 ± 5.48 fmol cell^{-1}, GTX4/1 24.87 ± 2.95 fmol cell^{-1}, neoSTX 2.89 ± 1.00 fmol cell^{-1}, and STX 0.60 ± 0.17 fmol cell^{-1} (Fig. 5).

In the case of MCS treatment, the first exposure showed GTX2/3 as the dominant toxin (17.46 ± 2.89 fmol cell^{-1}), followed by GTX4/1 (6.63 ± 1.51 fmol cell^{-1}), neoSTX (0.71 ± 0.23 fmol cell^{-1}), and STX

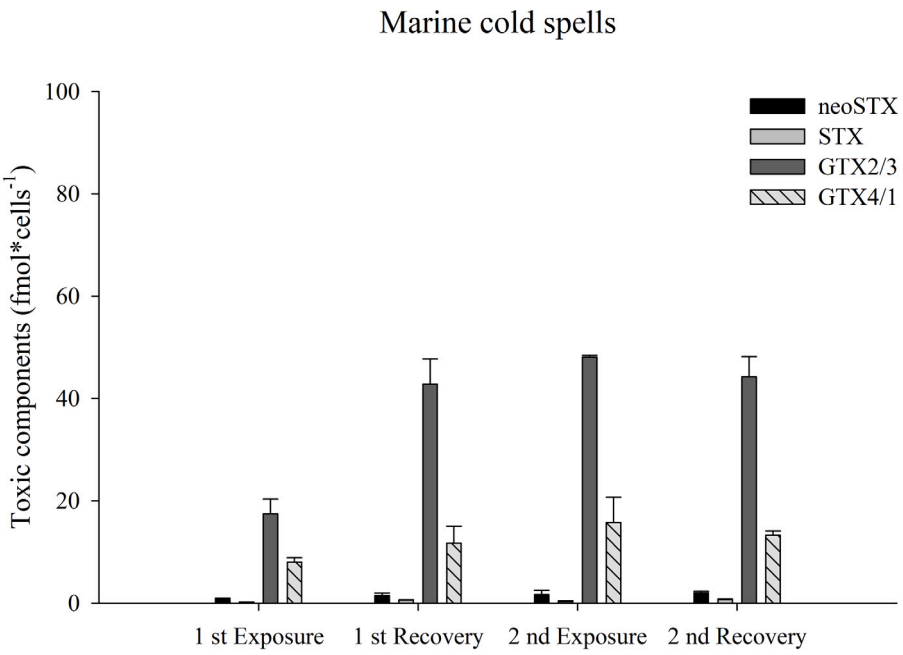

Fig. 6. Toxics components of *Alexandrium catenella* under simulated marine cold spells. Cellular toxin concentrations (fmol * cell^{-1}) of neoSTX, STX, GTX2/3 and GTX4/1 during two exposure–recovery cycles are depicted. Bar heights indicate mean values and error bars denote the standard error (SE).

(0.17 ± 0.04 fmol cell^{-1}). In the first recovery, GTX2/3 increased to 42.81 ± 4.92 fmol cells^{-1}, while GTX4/1, neoSTX, and STX reached 11.70 ± 3.35, 1.49 ± 0.47, and 0.57 ± 0.05 fmol cells^{-1}, respectively. The second MCSs exposure produced a slight increase in GTX2/3 (48.11 ± 4.92 fmol cells^{-1}), with GTX4/1 at 15.76 ± 4.93, neoSTX at 1.65 ± 0.87, and STX declining to 0.30 ± 0.13 fmol cells^{-1}. During the second recovery, GTX2/3 remained predominant (44.23 ± 3.96 fmol cells^{-1}), while GTX4/1, neoSTX, and STX reached 13.29 ± 0.82, 2.00 ± 0.29, and 0.67 ± 0.13 fmol cells^{-1}, respectively (Fig. 6).

For the control treatment, GTX2/3 remained the dominant toxin throughout the experiment. On day 9 (coinciding with the first exposure of MHWs/MCSs), the concentrations reached 25.72 ± 3.27 fmol cell^{-1}, followed by GTX4/1 (7.98 ± 1.87 fmol cell^{-1}), neoSTX (1.24 ± 0.40 fmol cell^{-1}) and STX (0.50 ± 0.06 fmol cell^{-1}). By day 18 (first recovery), GTX2/3 increased to 34.02 ± 2.74, GTX4/1 to 25.36 ± 3.15, neoSTX to 2.32 ± 0.56, while STX decreased to 0.21 ± 0.06 fmol cell^{-1}. On day 31 (second exposure), similar values were observed, with GTX2/3 (28.83 ± 3.14), GTX4/1 (25.90 ± 2.10), neoSTX (3.93 ± 0.56), and STX (0.38 ± 0.11). Finally, on day 40 (second recovery), toxin production decreased slightly, but GTX2/3 remained dominant (23.09 ± 3.65), followed by GTX4/1 (22.13 ± 1.37), neoSTX (1.72 ± 0.23) and STX (0.10 ± 0.002 fmol cell^{-1}) (Fig. 7).

PERMANOVA revealed a statistically significant interactive effect of condition and exposure on toxin production (R^2 = 0.46; $F_{6,24}$ = 9.21; p = 0.001). For the control group, the largest between-stage difference that between the first exposure and first recovery (R^2 = 0.76; $F_{1,4}$ = 12.9)—the decrease in the concentration of GTX4/1 accounted for most of this difference (SIMPER contribution = 18%). Within the MHWs group, the largest difference was observed between the first and second exposure (R^2 = 0.818; $F_{1,4}$ = 18.0), mainly driven by the decrease in GTX2/3 concentration (SIMPER contribution = 32.9%). Similarly, under MCS conditions, the largest difference was also observed between the first and second exposure phases (R^2 = 0.812; $F_{1,4}$ = 17.37), but primarily associated with the increase in GTX2/3 (SIMPER contribution = 34.5%).

During the first exposure phase, the largest between-treatment difference occurred between MHW and control conditions (R^2 = 0.91; $F_{1,4}$ = 42.5), mainly due to increased GTX2/3 concentrations under MHW conditions. The effect of MCS during the first recovery phase was chiefly accounted for by the increase in GTX4/1 (12% contribution), and the effects of MCS during the second exposure and recovery phases were driven chiefly by increments in the concentrations of GTX2/3 (contributions to each contrast = 18.7% and 19.8%, respectively).

3.2. Chlorophyll-α and pheopigments

The LMM revealed a significant condition by exposure interactive effect on chlorophyll-*a* concentration ($F_{6,24}$ = 3.73, p = 0.009, R^2 = 0.665). Under MHW conditions, chlorophyll-*a* showed a marked increase during the first exposure, which differed significantly from subsequent exposure and recovery phases (Fig. 7, post-hoc test: $p < 0.001$ and p = 0.012, respectively). In the control treatment, chlorophyll-*a* concentrations remained relatively stable over time, although a slight and statistically non-significant (post-hoc test: $p > 0.9$) decrease was observed on days 31 and 40, corresponding to the second exposure and recovery phases. In the MCS group, exposure had no detectable influence on chlorophyll-*a* concentration (post-hoc test: $p > 0.8$). The between-condition comparison within each exposure stage indicated that, during the first exposure, MHW generated a significant increase in chlorophyll-*a* compared with the control (post-hoc test: $p < 0.001$)—during this stage, MCS had no statistically significant effect on chlorophyll-*a* relative to the control group (p = 0.53). During the other three experimental stages, we detected no statistically significant differences effect of MHW and MCS relative to the control (post-hoc test: $p > 0.2$).

Square root-transformed pheopigment concentrations also showed a significant interaction between condition and exposure (R^2 = 0.91; $F_{6,24}$ = 5.87, $p < 0.001$). Under control conditions, pheopigments increased significantly during the second exposure and recovery phases relative to the first exposure and recovery phases (post-hoc test: $p < 0.001$; Fig. 8). MHW treatments produced moderate temporal variation, whereas MCS conditions showed significantly higher pheopigment concentrations during the second recovery phase relative to all previous stages (post-hoc test: $p \leq 0.003$). Between-treatment comparisons indicated lower pheopigment concentrations under MCS relative to controls during the first and second exposure phases, whereas MHW differed from the control only during the second recovery stage.

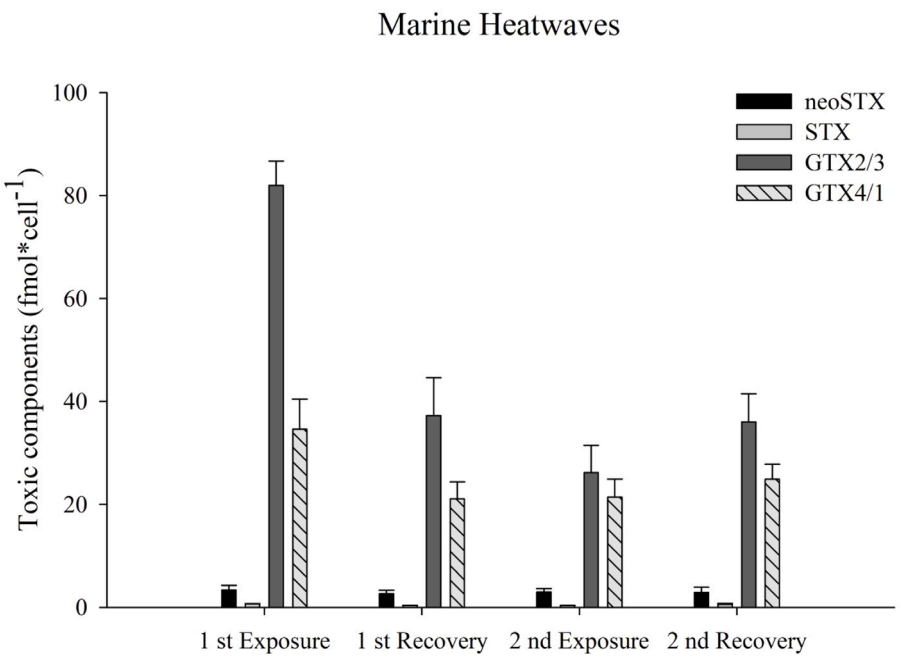

Fig. 7. Toxic components of *Alexandrium catenella* under simulated marine heatwaves. Cellular toxin concentrations (fmol * cell^{-1}) of neoSTX, STX, GTX2/3 and GTX4/1 during two exposure–recovery cycles are depicted. Bar heights indicate mean values and error bars denote the standard error (SE).

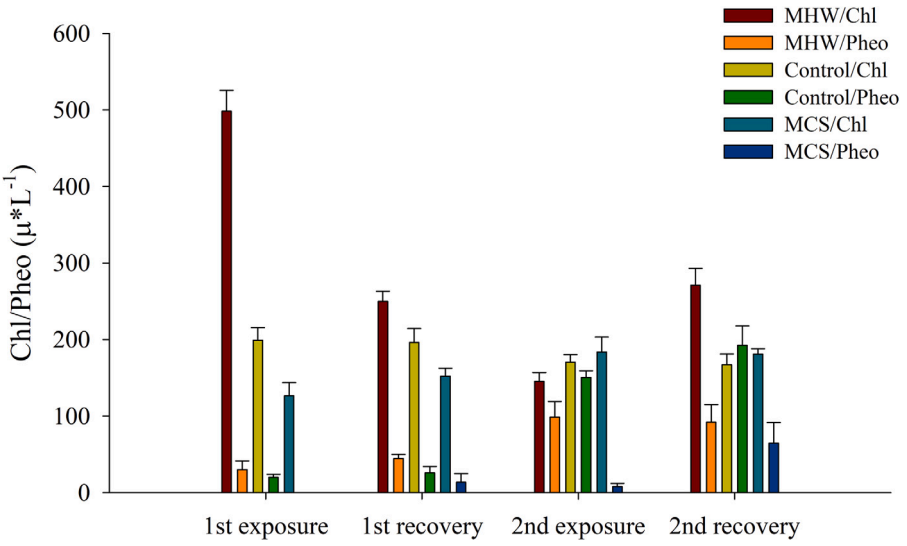

Fig. 8. Chlorophyll-*a* (Chl) and pheopigment (Pheo) concentrations (µg L^{-1}) in *Alexandrium catenella* under control, marine heatwaves, and marine cold spells experimental conditions across four phases: 1st exposure, 1st recovery, 2nd exposure, and 2nd recovery. Bar heights indicate mean values and error bars denote the standard error (SE).

4. Discussion

Our study provides experimental evidence that transient thermal extremes, simulating both marine heatwaves (MHWs) and marine cold spells (MCSs), can modify physiological responses in the monoclonal *Alexandrium catenella* strain examined here, particularly cell-density dynamics and cellular toxin production. Warming treatments were associated with increased GTX2/3 concentrations, whereas comparatively smaller changes were observed for GTX4/1. These findings indicate that transient thermal variability can influence the physiology and toxin profile of this strain under controlled laboratory conditions. Previous studies have suggested that MHWs and MCSs may also alter environmental and ecological processes, including mixed layer depth, nutrient availability, water column stratification, and grazing pressure, thereby modifying phytoplankton successional dynamics and potentially favoring communities dominated by harmful taxa. Similarly, proposed that climate driven environmental change may produce both "winners" and "losers" among HAB species, with *Alexandrium catenella* identified as one of the taxa potentially favored under several environmental scenarios relevant to Patagonian fjords. Nevertheless, because the present study was conducted using a single monoclonal culture under controlled laboratory conditions, the observed responses should not be directly extrapolated to natural populations, multispecies phytoplankton communities, or regional HAB dynamics. Future studies integrating multiple strains, field observations, and interacting environmental drivers will be necessary to evaluate the ecological relevance and generality of these responses.

Interannual environmental variability along the NW Patagonian coast is strongly modulated by large-scale climate modes, primarily

the El Niño–Southern Oscillation (ENSO) and the Southern Annular Mode (SAM) (Garreaud et al., 2009; Garreaud, 2018; Boisier et al., 2018). Periods of intense thermal variability have been linked to atmospheric and oceanic anomalies arising from interactions and at times synchrony between ENSO and SAM phases (Garreaud, 2018; Díaz et al., 2023). The regional climate is characterized by strong seasonality, with atmospheric temperatures ranging from 4–5°C in winter to 13–15°C in summer (Garreaud, 2018). Sea surface temperature (SST) follows a similar seasonal cycle, varying from 8–12°C in winter to 14–16°C in summer, superimposed on strong mesoscale variability driven by circulation and bathymetry (Narváez et al., 2019; Saldías et al., 2021). Additionally, satellite observations indicate a regional warming trend of 0.25°C per decade and a poleward displacement of upwelling-favorable winds during late summer (Narváez et al., 2019). Although northern Patagonia is classically described as hyper-humid, recent decades have seen precipitation deficits exceeding 50%, accompanied by enhanced solar radiation, particularly during synchronous ENSO–SAM phases (Garreaud, 2018; Pujol et al., 2022; Marquet et al., 2024). These conditions likely enhance thermohaline stratification and nutrient retention, creating favorable settings for atypical HAB development (León-Muñoz et al., 2018; Díaz et al., 2021). Indeed, our results suggest that warming conditions associated with MHWs stimulate toxin (GTX2/3) production and increase chlorophyll-a specifically during the first exposure phase in *A. catenella*, indicating that elevated temperatures may enhance both the toxicity and short-term physiological activity of this species.

Previous studies have shown that *Alexandrium catenella* reaches maximum growth rates within a relatively narrow thermal window of approximately 15–16°C (Navarro et al., 2006; Aguilera-Belmonte et al., 2013; Avila et al., 2015), whereas toxin content generally decreases with increasing temperature under steady-state laboratory conditions (Granéli and Flynn, 2006; Navarro et al., 2006). In contrast, our results demonstrate that transient exposure to elevated temperatures characteristic of marine heatwaves (MHWs) was associated with increased toxin content, particularly GTX2/3. This discrepancy suggests that toxin production may respond not only to temperature magnitude but also to the temporal dynamics of thermal stress, highlighting the importance of exposure–recovery cycles rather than static thermal thresholds alone.

Our findings are broadly consistent with observations from the extreme 2016 harmful algal bloom event in northern Patagonia, during which anomalous climatic conditions generated a prolonged MHW that, together with favorable local hydrodynamic conditions, supported exceptionally high *A. catenella* abundances (Pujol et al., 2022; Díaz et al., 2024). Likewise, Pujol et al. (2025) reported a positive association between MHW occurrence and *A. catenella* blooms in northern Patagonia, suggesting that elevated temperatures may enhance bloom development under suitable environmental conditions. Although our experimental results emphasize the role of thermal extremes, *A. catenella* dynamics are likely influenced by multiple interacting components of climate change. In particular, ocean warming, altered stratification, changes in freshwater discharge, and ocean acidification may act synergistically to modify bloom intensity and toxicity. For example, Tatters et al. (2013) demonstrated that elevated CO_2 concentrations can induce physiological responses in toxic dinoflagellates irrespective of nutrient status or temperature, indicating that ocean acidification may directly affect cellular metabolism and toxin production. Together, these findings suggest that future ocean conditions characterized by increasing thermal variability and elevated CO_2 levels may alter both the abundance and toxicity of *A. catenella*, potentially increasing the ecological and socioeconomic risks associated with harmful algal blooms in Patagonia and other temperate coastal ecosystems.

The toxin profile of *A. catenella* can vary among geographic regions and strains (Anderson et al., 2012). This species produces a diverse group of paralytic shellfish toxins (PSTs), including saxitoxin (STX), neosaxitoxin (neoSTX), and gonyautoxins (GTXs), whose relative proportions can substantially influence overall toxicity. Previous studies have shown that toxin profiles in *A. catenella* populations from Patagonia are commonly dominated by GTX and N-sulfocarbamoyl analogues, although substantial intra-specific variability exists among strains and geographic regions (Krock et al., 2007; Rodríguez-Villegas et al., 2021). Consistent with these observations, the toxin profile remained relatively stable across the experimental treatments and was consistently dominated by GTX analogues, particularly GTX2/3. Because GTX2/3 and GTX4/1 were quantified as combined epimeric pairs, and the individual analogues within each pair possess different toxicity equivalency factors (TEFs), conversion to saxitoxin equivalents (STX-eq) was not considered analytically appropriate. Consequently, the results are presented as molar cellular toxin profiles and should not be interpreted as direct estimates of neurotoxic potency or environmental toxic risk.

Despite the numerous studies describing toxin content and profiles in *Alexandrium catenella*, relatively few have examined how transient environmental stressors influence toxin production and composition. For example, Laabir et al. (2013) investigated the effects of environmental conditions on PST content and composition in a Mediterranean strain of *A. catenella* and found no significant changes in cellular toxin content under steady-state conditions. In contrast, our results indicate that short-term thermal anomalies can alter toxin dynamics. Simulated marine heatwave (MHW) conditions were associated with elevated GTX2/3 concentrations during the first exposure phase, whereas marine cold spell (MCS) conditions produced a delayed response, with peak GTX2/3 concentrations occurring during the second exposure–recovery cycle. In both treatments, GTX2/3 concentrations consistently exceeded those observed under control conditions.

Although the overall toxin profile remained relatively stable and continued to be dominated by GTX analogues, particularly GTX2/3, toxin content varied substantially among exposure and recovery phases. This pattern suggest that toxin production is influenced not only by temperature itself but also by the temporal dynamics of exposure and recovery. Such responses contrast with previous studies conducted under constant temperature conditions, which often reported an inverse relationship between temperature and toxin production (Navarro et al., 2006; Kim et al., 2021). Our findings therefore highlight the importance of transient thermal variability as a key regulator of toxicity, suggesting that short-term warming and cooling events may alter toxicity in ways that cannot be predicted from steady-state experiments alone. As marine heatwaves and other climatic extremes become increasingly frequent and intense, understanding how recurrent thermal fluctuations affect toxin production will be critical for improving HAB risk assessments and forecasting toxicity under future climate scenarios.

5. Conclusions

This study provides experimental evidence that transient thermal extremes, simulating marine heatwaves (MHWs) and marine cold spells (MCSs), can modify cell-density dynamics and cellular toxin production in a monoclonal strain of *Alexandrium catenella*. Warming treatments were associated with short-term increases in cell density and GTX2/3 concentrations, whereas comparatively smaller changes were observed under simulated cold-spell conditions. Despite these quantitative responses, the overall toxin profile remained relatively stable and continued to be dominated by GTX analogues.

These findings indicate that short-term thermal variability can influence the physiological performance of *A. catenella* under controlled laboratory conditions. However, because this study was conducted using a single monoclonal strain under simplified experimental conditions, the observed responses should not be directly extrapolated to natural populations, multispecies phytoplankton communities, or regional harmful algal bloom dynamics. Future studies incorporating multiple strains, natural populations, and interacting environmental drivers will be necessary to determine the generality and ecological significance of these responses under changing climate conditions.

CRediT authorship contribution statement

Paola A. Villanueva: Writing – review & editing, Writing – original draft, Visualization, Validation, Supervision, Software, Resources, Project administration, Methodology, Investigation, Funding acquisition, Formal analysis, Data curation, Conceptualization. **Carlos Lara:** Writing – review & editing, Writing – original draft, Visualization, Validation, Supervision, Software, Resources, Methodology, Investigation, Funding acquisition, Formal analysis, Conceptualization. **Jorge M. Navarro:** Writing – review & editing, Writing – original draft, Visualization, Supervision, Resources, Methodology, Funding acquisition, Conceptualization. **Nelson Valdivia:** Writing – review & editing, Writing – original draft, Validation, Formal analysis. **Elisabeth Teca:** Writing – original draft, Visualization, Validation, Software, Project administration, Methodology, Investigation, Formal analysis, Data curation, Conceptualization. **Amália M.S. Detoni:** Writing – review & editing, Writing – original draft. **Gonzalo S. Saldías:** Writing – review & editing, Writing – original draft, Funding acquisition, Data curation. **Pamela Carbonell:** Writing – review & editing, Writing – original draft, Funding acquisition, Formal analysis. **Luis Norambuena:** Visualization, Methodology, Formal analysis. **Patricio A. Díaz:** Writing – review & editing, Writing – original draft, Visualization, Validation, Methodology, Investigation, Funding acquisition. **Bernardo R. Broitman:** Writing – review & editing, Writing – original draft, Funding acquisition, Data curation.

Declaration of competing interest

The authors declare that they have no known competing financial interests or personal relationships that could have appeared to influence the work reported in this paper.

Acknowledgments

This study was supported by the Chilean National Research and Development Agency (ANID) through the National PhD Fellowship 212102252 awarded to PA-V. J.M.N., P.A.V., and N.V. were supported by the Center FONDAP-IDEAL (Grant No. 15150003). C.L. was supported by FONDECYT Grant 1230420. Gonzalo S. Saldías has been partially supported by COPAS Coastal ANID FB210021. B.R.B. was supported by FONDECYT Grant 1221699 and the Instituto Milenio en Socio-Ecología Costera (SECOS; ICN2019-015). P.A.D. was supported by FONDECYT Grant 1231220 and Centro Interdisciplinario para la Investigación Acuícola — Investigación Aplicada (INCAR2), CIA250009, ANID, Chile. N.V. was also supported by FONDECYT Grant 1230286.

Data availability

Data will be made available on request.

References

Aguilera-Belmonte, A., Inostroza, I., Carrillo, K.S., Franco, J.M., Riobó, P., Gómez, P.I., 2013. The combined effect of salinity and temperature on the growth and toxin content of four Chilean strains of *Alexandrium catenella* (Whedon and Kofoid) Balech 1985 (Dinophyceae) isolated from an outbreak occurring in southern Chile in 2009. Harmful Algae 23, 55–59.

Anderson, D.M., Alpermann, T.J., Cembella, A.D., Collos, Y., Masseret, E., Montresor, M., 2012. The globally distributed genus *Alexandrium*: Multifaceted roles in marine ecosystems and impacts on human health. Harmful Algae 14, 10–35.

Avdelas, L., Avdic-Mravlje, E., Borges Marques, A.C., Cano, S., Capelle, J.J., Carvalho, N., Cozzolino, M., Dennis, J., Ellis, T., Fernández Polanco, J.M., et al., 2021. The decline of mussel aquaculture in the European union: Causes, economic impacts and opportunities. Rev. Aquac. 13 (1), 91–118.

Avila, M., De Zarate, C., Clement, A., Carbonell, P., Pérez, F., 2015. Efecto de factores abióticos en el crecimiento vegetativo de *Alexandrium catenella* proveniente de quistes en laboratorio. Rev. Biol. Mar. Oceanogr. 50, 177–185.

Barría, C., Vásquez-Calderón, P., Lizama, C., Herrera, P., Canto, A., Conejeros, P., Beltrami, O., Suárez-Isla, B.A., Carrasco, D., Rubilar, I., et al., 2022. Spatial temporal expansion of harmful algal blooms in Chile: A review of 65 years records. J. Mar. Sci. Eng. 10 (12), 1868.

Bill, B.D., Moore, S.K., Hay, L.R., Anderson, D.M., Trainer, V.L., 2016. Effects of temperature and salinity on the growth of *Alexandrium* (Dinophyceae) isolates from the Salish sea. J. Phycol. 52 (2), 230–238.

Boisier, J.P., Alvarez-Garreton, C., Cordero, R.R., Damiani, A., Gallardo, L., Garreaud, R.D., Lambert, F., Ramallo, C., Rojas, M., Rondanelli, R., 2018. Anthropogenic drying in central-southern Chile evidenced by long-term observations and climate model simulations. Elementa Sci. Anthopocene 6, 74.

Bui, Q.T.N., Pradhan, B., Kim, H.-S., Ki, J.-S., 2024. Environmental factors modulate saxitoxins (STXs) production in toxic dinoflagellate *Alexandrium*: An updated review of STXs and synthesis gene aspects. Toxins 16 (5), 210.

Burgh-Day, C.O.D., Spillman, C.M., Smith, G., Stevens, C.L., 2022. Forecasting extreme marine heat events in key aquaculture regions around New Zealand. J. South. Hemisph. Earth Syst. Sci. 72, 58–72.

Cembella, A.D., 1998. Ecophysiology and metabolism of paralytic shellfish toxins in marine microalgae. Physiol. Ecol. Harmful Alga Bloom. 381–403.

Chakraborty, S., Pančić, M., Andersen, K.H., Kiørboe, T., 2019. The cost of toxin production in phytoplankton: The case of PST producing dinoflagellates. ISME J. 13 (1), 64–75.

Cuevas, L.A., Tapia, F.J., Iriarte, J.L., González, H.E., Silva, N., Vargas, C.A., 2019. Interplay between freshwater discharge and oceanic waters modulates phytoplankton size-structure in fjords and channel systems of the Chilean Patagonia. Prog. Oceanogr. 173, 103–113.

Deschaseaux, E., O'brien, J., Siboni, N., Petrou, K., Seymour, J.R., 2019. Shifts in dimethylated sulfur concentrations and microbiome composition in the red-tide causing dinoflagellate *Alexandrium minutum* during a simulated marine heatwave. Biogeosciences 16 (22), 4377–4391.

Dias, M., Özkan, B., Ramos, J., Marques, A., Rosa, R., Costa, P.R., Maulvault, A.L., 2025. Hot and toxic: Accumulation dynamics and ecotoxicological responses of mussel *Mytilus galloprovincialis* exposed to marine biotoxins during a marine heatwave. Marine Poll. Bull. 213.

Díaz, P.A., Álvarez, G., 2023. Effects of microalgal blooms on aquaculture and fisheries. Fishes 8 (9), 461.

Díaz, P.A., Figueroa, R.I., 2023. Toxic algal bloom recurrence in the era of global change: Lessons from the Chilean Patagonian fjords. Microorganisms 11 (8), 1874.

Díaz, P.A., Gormaz, R., Aguayo, P., Pérez-Santos, I., Saldías, G.S., Figueroa, R.I., Fernández, P.A., Álvarez, G., Rodríguez-Villegas, C., Schwerter, C., et al., 2025. Unveiling the 2017 *Karenia* Bloom in NW Chilean Patagonia by integrating remote sensing and field data. Microorganisms 13 (11), 2440.

Díaz, P.A., Peréz-Santos, I., Álvarez, G., Garreaud, R., Pinilla, E., Díaz, M., Sandoval, A., Araya, M., Álvarez, F., Rengel, J., et al., 2021. Multiscale physical background to an exceptional harmful algal bloom of *Dinophysis acuta* in a fjord system. Sci. Total Environ. 773, 145621.

Díaz, P.A., Pérez-Santos, I., Basti, L., Garreaud, R., Pinilla, E., Barrera, F., Tello, A., Schwerter, C., Arenas-Uribe, S., Soto-Riquelme, C., et al., 2023. The impact of local and climate change drivers on the formation, dynamics, and potential recurrence of a massive fish-killing microalgal bloom in Patagonian fjord. Sci. Total Environ. 865, 161288.

Díaz, P.A., Rosales, S.A., Molinet, C., Niklitschek, E.J., Marín, A., Varela, D., Seguel, M., Díaz, M., Figueroa, R.I., Basti, L., et al., 2024. Are *Alexandrium catenella* blooms spreading offshore in southern Chile? An in-depth analysis of the first PSP outbreak in the Oceanic Coast. Fishes 9 (9), 340.

Garrabou, J., Gómez-Gras, D., Medrano, A., Cerrano, C., Ponti, M., Schlegel, R., Bensoussan, N., Turicchia, E., Sini, M., Gerovasileiou, V., et al., 2022. Marine heatwaves drive recurrent mass mortalities in the Mediterranean Sea. Global Change Biol. 28 (19), 5708–5725.

Garreaud, R., 2018. Record-breaking climate anomalies lead to severe drought and environmental disruption in western Patagonia in 2016. Clim. Res. 74 (3), 217–229.

Garreaud, R.D., Vuille, M., Compagnucci, R., Marengo, J., 2009. Present-day south American climate. Palaeogeogr. Palaeoclimatol. Palaeoecol. 281 (3–4), 180–195.

Granéli, E., Flynn, K., 2006. Chemical and physical factors influencing toxin content. In: Ecology of Harmful Algae. Springer.

Guillard, R.R., 1995. Culture methods. Man. Harmful Mar. Microalgae.

Han, M., Lee, H., Anderson, D.M., Kim, B., 2016. Paralytic shellfish toxin production by the dinoflagellate *Alexandrium pacificum* (Chinhae Bay, Korea) in axenic, nutrient-limited chemostat cultures and nutrient-enriched batch cultures. Marine Poll. Bull. 104 (1–2), 34–43.

Hernández, C., Díaz, P., Molinet, C., Seguel, M., 2016. Exceptional climate anomalies and northwards expansion of paralytic shellfish poisoning outbreaks in southern Chile. Harmful Algae News 54 (1).

Hobday, A.J., Alexander, L.V., Perkins, S.E., Smale, D.A., Straub, S.C., Oliver, E.C., Benthuysen, J.A., Burrows, M.T., Donat, M.G., Feng, M., et al., 2016. A hierarchical approach to defining marine heatwaves. Prog. Oceanogr. 141, 227–238.

Holbrook, N.J., Scannell, H.A., Sen Gupta, A., Benthuysen, J.A., Feng, M., Oliver, E.C., Alexander, L.V., Burrows, M.T., Donat, M.G., Hobday, A.J., et al., 2019. A global assessment of marine heatwaves and their drivers. Nat. Commun. 10 (1), 2624.

Kim, H., Park, H., Wang, H., Yoo, H.Y., Park, J., Ki, J.-S., 2021. Low temperature and cold stress significantly increase saxitoxins (STXs) and expression of STX biosynthesis genes sxtA4 and sxtG in the dinoflagellate *Alexandrium catenella*. Mar. Drugs 19 (6), 291.

Krock, B., Seguel, C.G., Cembella, A.D., 2007. Toxin profile of *Alexandrium catenella* from the Chilean coast as determined by liquid chromatography with fluorescence detection and liquid chromatography coupled with tandem mass spectrometry. Harmful Algae 6 (5), 734–744.

Laabir, M., Collos, Y., Masseret, E., Grzebyk, D., Abadie, E., Savar, V., Sibat, M., Amzil, Z., 2013. Influence of environmental factors on the paralytic shellfish toxin content and profile of *Alexandrium catenella* (Dinophyceae) isolated from the Mediterranean sea. Mar. Drugs 11 (5), 1583–1601.

Lara, C., Saldías, G.S., Tapia, F.J., Iriarte, J.L., Broitman, B.R., 2016. Interannual variability in temporal patterns of Chlorophyll–A and their potential influence on the supply of mussel larvae to inner waters in northern Patagonia (41–44 °s). J. Mar. Syst. 155, 11–18.

León-Muñoz, J., Urbina, M.A., Garreaud, R., Iriarte, J.L., 2018. Hydroclimatic conditions trigger record harmful algal bloom in western Patagonia (summer 2016). Sci. Rep. 8 (1), 1330.

Marquet, P.A., Buschmann, A.H., Corcoran, D., Díaz, P.A., Fuentes-Castillo, T., Garreaud, R., Pliscoff, P., Salazar, A., 2024. Global change and acceleration of anthropic pressures on patagonian ecosystems. In: Conservation in Chilean Patagonia: Assessing the State of Knowledge, Opportunities, and Challenges. Springer International Publishing Cham, pp. 33–65.

Molinet, C., Soto, D., León-Muñoz, J., Díaz, M., Espinoza, K., Henríquez, J., Matamala, T., 2025. Climate-driven changes in freshwater inputs to a northern patagonia Fjord and overfishing of wild mussel seed could threaten Chilean mussel farming. Clim. Change 178 (6), 119.

Moore, S.K., Trainer, V.L., Mantua, N.J., Parker, M.S., Laws, E.A., Backer, L.C., Fleming, L.E., 2008. Impacts of climate variability and future climate change on harmful algal blooms and human health. Environ. Health 7 (Suppl 2), S4.

Narváez, D.A., Vargas, C.A., Cuevas, L.A., García-Loyola, S.A., Lara, C., Segura, C., Tapia, F.J., Broitman, B.R., 2019. Dominant scales of subtidal variability in coastal hydrography of the northern Chilean Patagonia. J. Mar. Syst. 193, 59–73.

Navarro, J., Muñoz, M., Contreras, A., 2006. Temperature as a factor regulating growth and toxin content in the dinoflagellate *Alexandrium catenella*. Harmful Algae 5 (6), 762–769.

Navarro, J.M., Oyarzún, P.A., Haarmann, V., Toro, J.E., Garrido, C., Valenzuela, A., Pizarro, G., 2022. Feeding response and dynamic of intoxication and detoxification in two populations of the flat oyster *Ostrea chilensis* exposed to paralytic shellfish toxins (PST). Mar. Environ. Res. 177, 105634.

Oliver, E.C., Benthuysen, J.A., Darmaraki, S., Donat, M.G., Hobday, A.J., Holbrook, N.J., Schlegel, R.W., Sen Gupta, A., 2021. Marine heatwaves. Annu. Rev. Mar. Sci. 13 (1), 313–342.

Parsons, T., Maita, Y., 1984. Lalli C MA Manual of Chemical and Biological Methods for Seawater Analysis. Pergamon Press, pp. 109–115.

Pinillos, F.J.V., Ruiz, J.A.C., 2024. Coastal management and climate change on the island and the sea of Chiloé (Chile): An evaluation of policies, regulations, and instruments. Environ. Sci. Policy 156, 103758.

Poblete-Ulloa, J., Gutiérrez, M.H., Lange, C.B., Narváez, D.A., Montero, P., González, H.E., Fernández, C., 2024. Freshwater discharge drives latitudinal changes of phytoplankton composition on the continental shelf off Chilean Patagonia. J. Mar. Syst. 245, 103993.

Pujol, C., Barth, A., Pérez-Santos, I., Muñoz-Linford, P., Alvera-Azcárate, A., 2025. Overcoming challenges in coastal marine heatwave detection: Integrating *In Situ* and satellite data in Complex Coastal environment. EGUsphere 2025, 1–35.

Pujol, C., Pérez-Santos, I., Barth, A., Alvera-Azcárate, A., 2022. Marine heatwaves offshore central and south Chile: Understanding forcing mechanisms during the years 2016–2017. Front. Mar. Sci. 9, 800325.

Ritger, A.L., Hofmann, G.E., 2025. Bringing heatwaves into the lab: A low-cost, open-source, and automated system to simulate realistic warming events in an experimental setting. Limnol. Ocean.: Methods 23 (2), 87–96.

Rodriguez, I., Alfonso, A., Gonzalez-Jartin, J.M., Vieytes, M.R., Botana, L.M., 2018. A single run UPLC-MS/MS method for detection of all EU-regulated marine toxins. Talanta 189, 622–628.

Rodríguez, G.R., Villasante, S., do Carme García-Negro, M., 2011. Are red tides affecting economically the commercialization of the galician (NW Spain) mussel farming? Mar. Policy 35 (2), 252–257.

Rodríguez-Villegas, C., Díaz, P.A., Riobó, P., Rossignoli, A.E., Rodríguez, F., Loures, P., Baldrich, Á.M., Varela, D., Sandoval-Sanhueza, A., Figueroa, R.I., 2021. Latitudinal variation in the toxicity and sexual compatibility of *Alexandrium catenella* strains from southern Chile. Toxins 13 (12), 900.

Saldías, G.S., Hernández, W., Lara, C., Muñoz, R., Rojas, C., Vásquez, S., Pérez-Santos, I., Soto-Mardones, L., 2021. Seasonal variability of SST fronts in the inner sea of Chiloé and its adjacent coastal ocean, northern Patagonia. Remote. Sens. 13 (2), 181.

Schlegel, R.W., Oliver, E.C., Wernberg, T., Smit, A.J., 2017. Nearshore and offshore co-occurrence of marine heatwaves and cold-spells. Prog. Oceanogr. 151, 189–205.

Shimizu, Y., 1996. Microalgal metabolites: A new perspective. Annu. Rev. Microbiol. 50 (1), 431–465.

Smale, D.A., Wernberg, T., Oliver, E.C., Thomsen, M., Harvey, B.P., Straub, S.C., Burrows, M.T., Alexander, L.V., Benthuysen, J.A., Donat, M.G., et al., 2019. Marine heatwaves threaten global biodiversity and the provision of ecosystem services. Nat. Clim. Chang. 9 (4), 306–312.

Smith, K.E., Burrows, M.T., Hobday, A.J., King, N.G., Moore, P.J., Sen Gupta, A., Thomsen, M.S., Wernberg, T., Smale, D.A., 2023. Biological impacts of marine heatwaves. Annu. Rev. Mar. Sci. 15 (1), 119–145.

Smith, K.E., Burrows, M.T., Hobday, A.J., Sen Gupta, A., Moore, P.J., Thomsen, M., Wernberg, T., Smale, D.A., 2021. Socioeconomic impacts of marine heatwaves: Global issues and opportunities. Science 374 (6566), eabj3593.

Tatters, A.O., Flewelling, L.J., Fu, F., Granholm, A.A., Hutchins, D.A., 2013. High CO2 promotes the production of paralytic shellfish poisoning toxins by *Alexandrium catenella* from Southern California waters. Harmful Algae 30, 37–43.

Thompson, R.M., Beardall, J., Beringer, J., Grace, M., Sardina, P., 2013. Means and extremes: Building variability into community-level climate change experiments. Ecol. Lett. 16 (6), 799–806.

Utermohl, H., 1958. Zur Vervollkommung der quantitativen phytoplankton-methodik. Mitt Int. Limnol. 9, 38.

Van Dolah, E.R., Paolisso, M., Sellner, K., Place, A., 2016. Employing a socio-ecological systems approach to engage harmful algal bloom stakeholders. Aquat. Ecol. 50 (3), 577–594.

Villalobos, V.I., Morales-Torres, D.F., Valdivia, N., Rivera-Hechem, M.I., Giesecke, R., Pinones, A., Mardones, J.I., Garces-Vargas, J., Segura, C.J., Navarro, J.M., et al., 2025. Responses of mussel farms to harmful algal bloom governance are shaped by the scale of production: Implications for equitable blue economy. Harmful Algae 144, 102821.

Wells, M.L., Trainer, V.L., Smayda, T.J., Karlson, B.S., Trick, C.G., Kudela, R.M., Ishikawa, A., Bernard, S., Wulff, A., Anderson, D.M., et al., 2015. Harmful algal blooms and climate change: Learning from the past and present to forecast the future. Harmful Algae 49, 68–93.

Wiese, M., D'Agostino, P.M., Mihali, T.K., Moffitt, M.C., Neilan, B.A., 2010. Neurotoxic alkaloids: Saxitoxin and its analogs. Mar. Drugs 8 (7), 2185–2211.

Zhu, J., Cai, Y., Wakisaka, M., Yang, Z., Yin, Y., Fang, W., Xu, Y., Omura, T., Yu, R., Zheng, A.L.T., 2023. Mitigation of oxidative stress damage caused by abiotic stress to improve biomass yield of microalgae: A review. Sci. Total Environ. 896, 165200.